

Article

Research on the Energy-Saving Strategy of Path Planning for Electric Vehicles Considering Traffic Information

Guanghai Zhu ^{1,2}, Jianbin Lin ^{1,*}, Qingwu Liu ¹ and Hongwen He ^{1,*} 

¹ National Engineering Laboratory for Electric Vehicles, School of Mechanical Engineering, Beijing Institute of Technology, Beijing 100081, China; Zhugh@yutong.com (G.Z.); qinwoodliu@163.com (Q.L.)

² Zhengzhou Yutong Bus Co., Ltd., Yutong Industry Park, Yutong Road, Zhengzhou 450017, China

* Correspondence: bitlinjb@163.com (J.L.); hwhebit@bit.edu.cn (H.H.); Tel.: +86-10-6891-4842 (H.H.)

Received: 14 July 2019; Accepted: 13 September 2019; Published: 20 September 2019



Abstract: Battery-powered electric vehicles (EVs) have a limited on-board energy storage and present the problem of driving mileage anxiety. Moreover, battery energy storage density cannot be effectively improved in a short time, which is a technical bottleneck of EVs. By considering the impact of traffic information on energy consumption forecasting, an energy-saving path planning method for EVs that takes traffic information into account is proposed. The modeling process of the EV model and the construction process of the traffic simulation model are expounded. In addition, the long-term, short-term memory neural network (LSTM) model is selected to predict the energy consumption of EVs, and the sequence to sequence technology is used in the model to integrate the driving condition data of EVs with traffic information. In order to apply the predicted energy consumption to travel guidance, a road planning method with the optimal coupling of energy consumption and distance is proposed. The experimental results show that the energy-based economic path uses 9.9% lower energy consumption and 40.2% shorter travel time than the distance-based path, and a 1.5% lower energy consumption and 18.6% longer travel time than the time-based path.

Keywords: energy consumption prediction; deep learning; path planning; energy-saving strategy; battery electric vehicle

1. Introduction

The development of electric vehicles (EVs) can effectively solve environmental pollution, improve urban air quality, and alleviate energy shortage pressure [1,2]. However, the drivers are often plagued by EV mileage anxiety, which affects the driving experience due to the limitation of power battery capacity and worrying about the unknown energy consumption on future road segments [3]. The driving range of the remaining energy of the power battery is generally estimated based on the new european driving cycle (NEDC) [4] and the path planning method commonly used in EVs in travel navigation is based on the shortest travel route [5]. The disadvantage of this method is that NEDCs are different from the actual traffic conditions [6] and the occupants cannot know whether the remaining energy is enough to reach the destination. In daily travel, the shortest path may result in wasted energy consumption of EVs due to traffic congestion and, therefore, the travel time will also increase [7,8].

To effectively reduce energy consumption and improve driving range, previous research on the energy management of EVs have investigated nonlinear model predictive control [9], multi-objective optimization [10], RBF-neural network [11], estimation of preceding vehicle future movements [12], global optimization [13], and deep learning [14]; however, the above-mentioned papers neglect the influence of the actual traffic conditions. To solve such problems, a new modal activity framework for

vehicle energy/emissions estimation using sparse mobile sensor data is presented in reference [15] and a data-driven model is built to estimate EV energy consumption on each roadway link considering real-world traffic conditions in reference [16]. For the complicated energy system of a plug-in hybrid electric vehicle, a generic framework of an online energy management system that is based on an evolutionary algorithm is proposed and can achieve the best fuel economy improvement, which require less trip information in reference [17]. It is possible to predict future energy consumption based on the vehicle historical states and predict the remaining driving range more accurately based on the future driving conditions under the help of traffic information.

In this paper, based on the information of a traffic network, the driving conditions of EVs are fully considered to accurately predict the energy consumption and the problem of the energy-saving path with optimal coupling of energy consumption and distance is discussed and the solution method is explored with the aim being to effectively alleviate mileage anxiety. Finally, the travel time and travel energy consumption are reasonably reduced, while the accuracy and effectiveness of the method are verified by simulation experiments.

The article structure is arranged in seven sections. Section 2 builds the models of the battery-powered electric car and then verifies the models with experimental data. Section 3 builds the models of the traffic network. Section 4 puts forward an LSTM model to perform the prediction of energy consumption and sequence to sequence technology is used in the model to integrate the driving condition data of EVs with the traffic information based on the models built in Sections 2 and 3. Section 5 gives a planning strategy for an optimal coupling path between energy consumption and distance. Section 6 performs three kinds of experiments: distance-based, energy-based, and time-based optimal simulations, and provides the results. Section 7 lists the main conclusions.

2. Battery-Powered Electric Vehicle Modeling

In order to accurately obtain the driving energy consumption, a battery-powered EV model is built based on the EU260 electric car. The EV model includes a driver model, driving system model, power battery model, and vehicle dynamics model [18–21].

2.1. Driver Model

A proportional-integral-derivative controller (PID) is used to model the driver to accurately follow the actual vehicle speed with the desired speed as shown in Equation (1) [19].

$$P_{acc} = \frac{1}{P_{ed}} \left(K_p v_e + \alpha_i K_i \int_0^t v_e dt \right) \times 100\% \quad (1)$$

$$v_e = v_{pre} - v_{act} \quad (2)$$

$$\alpha_i = \begin{cases} 0, & \left| K_i \int_0^t v_e dt \right| > P_{ed} \\ 1, & \left| K_i \int_0^t v_e dt \right| \leq P_{ed} \end{cases} \quad (3)$$

where v_{pre} is the expected speed, v_{act} is the actual speed, v_e is the difference between the actual speed and the expected speed, α_i is the integral anti-saturation parameter of the PID regulator, K_p is the proportional parameter of PID, K_i is the integral parameter of PID, and P_{acc} is the depth of the accelerator pedal or brake pedal, P_{ed} is the full-scale depth of the accelerator pedal or brake pedal with the value range of $[-100\%, 100\%]$. If P_{acc} is negative, it means that the EV is braking. If it is positive, it means the EV is speeding up [22,23].

2.2. Driving System Model

The vehicle driving model is built with Equations (4)–(7)

$$F_{\text{tra}} = T_{\text{out}}\eta_{\text{wheel}}/r \quad (4)$$

$$T_{\text{out}} = P_{\text{acc}}T_{\text{max}} \quad (5)$$

$$T_{\text{motor}} = T_{\text{out}}/\eta_t \quad (6)$$

$$P_{\text{motor}} = T_{\text{motor}}\omega_{\text{motor}} \quad (7)$$

where F_{tra} is the driving force of the tire, r is the tire rolling radius of the driving wheel, T_{out} is the output torque of the motor drive system, η_{wheel} is the transmission efficiency between the drive system and the wheel, $\eta_{\text{wheel}} = 98\%$, and T_{max} is the maximum torque that the motor drive system can output, the peak power of the driving motor is 100 kW and its maximum torque is 265 Nm. T_{motor} is the output torque of the driving motor, η_t is the efficiency of the motor drive system, P_{motor} is the output power of the driving motor, and ω_{motor} is the output speed of the driving motor.

2.3. Power Battery Model

The Rint circuit model is selected as the equivalent circuit model of the power battery [20]. The Rint model consists of an ideal voltage source and a resistor [24].

$$P_{\text{batt}} = P_{\text{motor}}/\eta_m \quad (8)$$

$$P_{\text{batt}} = U_{\text{oc}}I_L - I_L^2R_0 \quad (9)$$

$$I_L = \frac{U_{\text{oc}} - \sqrt{U_{\text{oc}}^2 - 4R_0P_{\text{batt}}}}{2R_0} \quad (10)$$

$$\text{SOC}_t = \text{SOC}_0 - \frac{\int_0^t \eta_{\text{batt}}I_L dt}{Q_b} \quad (11)$$

where P_{batt} is the battery output power, η_m is the efficiency of the driving motor system including motor and motor controller, which can be obtained by the look-up table method based on the efficiency map shown as Figure 1; U_{oc} is the battery open-circuit voltage, I_L is the battery operating current, R_0 is the battery internal resistance, and here U_{oc} and R_0 can be measured with the experimental method [25]. SOC_t is the SOC to be solved, SOC_0 is the initial value of the power battery SOC, Q_b is the total capacity of the power battery, which decreases with the decrease of a battery state of health (SOH) [21], η_{batt} is the power battery charge and discharge efficiency.

$$\eta_{\text{batt}} = \begin{cases} 98\%, I_L < 0 \\ 100\%, I_L \geq 0 \end{cases} \quad (12)$$

When the battery is charging ($I_L < 0$), $\eta_{\text{batt}} = 98\%$, and when the battery is in discharging ($I_L \geq 0$), $\eta_{\text{batt}} = 100\%$.

The SOC of the power battery can be solved according to the above Equation (10).

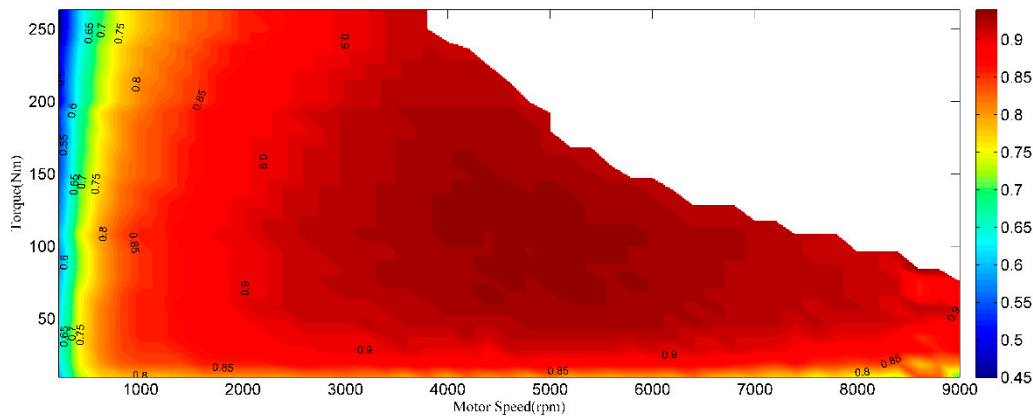


Figure 1. Efficiency map of the electric vehicle (EV) driving motor system.

2.4. Vehicle Driving Dynamics Model

The vehicle driving dynamics model was built with Equations (13)–(16)

$$F_{\text{tra}} = F_g + F_r + F_a + \delta m a \quad (13)$$

$$F_g = m g \sin \theta \quad (14)$$

$$F_r = m g \cos \theta C_r \quad (15)$$

$$F_a = \frac{1}{2} \rho_a C_a A_f v^2 \quad (16)$$

where m is the total mass of the EV, δ is the equivalent coefficient of the EV moment inertia, a is the EV acceleration rate, F_{tra} is the driving force, F_g is the gravity resistance along the road surface, F_r is the rolling resistance, and F_a is the air resistance. g is the gravitational acceleration, θ is the road gradient, and C_r is the tire rolling resistance coefficient. ρ_a is the air density, C_a is the air resistance coefficient, A_f is the windward area of the EV, and v is the EV speed.

2.5. Verification of the Accuracy of the EV Model

The accuracy of the vehicle model is verified through the energy consumption comparison between the simulation and experiment, the driving cycle input is designed as the 3 continuous NEDC driving cycles on the test bench [26] and an actual road driving cycle as shown in Figure 2a,b.

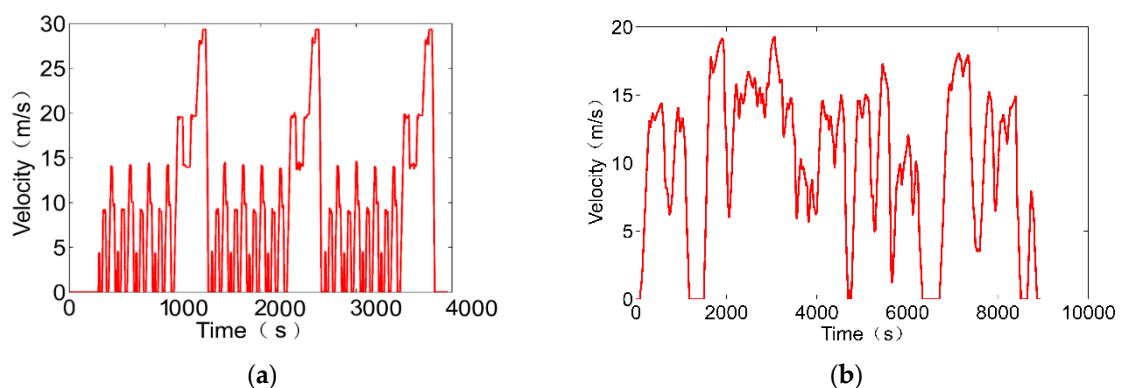


Figure 2. Two driving cycles to verify the accuracy of the EV model: (a) the 3 new energy driving cycles (NEDCs) on the test bench; (b) the actual road driving cycle.

After the three NEDCs shown in Figure 2a, the real vehicle consumes 11.8% of the total energy and the model consumes 12.1% of the total energy with an error of 0.3% as listed in Table 1.

Table 1. Comparison of energy consumption between the real vehicle and the model for 3 NEDCs.

Vehicle Type	Driving Condition	Energy Consumption
Real Vehicle	3 NEDCs on test bench	11.8%
Model	3 NEDCs input	12.1%

As listed in Table 2, after running 8939 s on an actual road as shown in Figure 2b, the real vehicle runs for 18.01 km and consumes 7.0% of the total energy and the model consumes 7.2% of the total energy with an error of 2.8%.

Table 2. Comparison of energy consumption between the real vehicle and the model for actual road driving.

Vehicle Type	Driving Condition	Energy Consumption
Real Vehicle	Actual road driving	7.0%
Model	Actual road driving cycle input	7.2%

According to the above two conditions, it can be considered that the vehicle model has enough accuracy when calculating energy consumption.

3. Modeling of the Traffic Network

The SUMO (Simulation of Urban Mobility) [27] high-precision urban traffic simulation software is used to simulate the traffic network. The main task is to layout and plan the roads and intersections, then use the actual observation data to design the traffic parameters. Based on the traffic network of the Chaoyang District of Beijing, which is about 4 km long and about 5 km wide, a total of 20 km² regions, the traffic network simulation model is established, as shown in Figure 3.

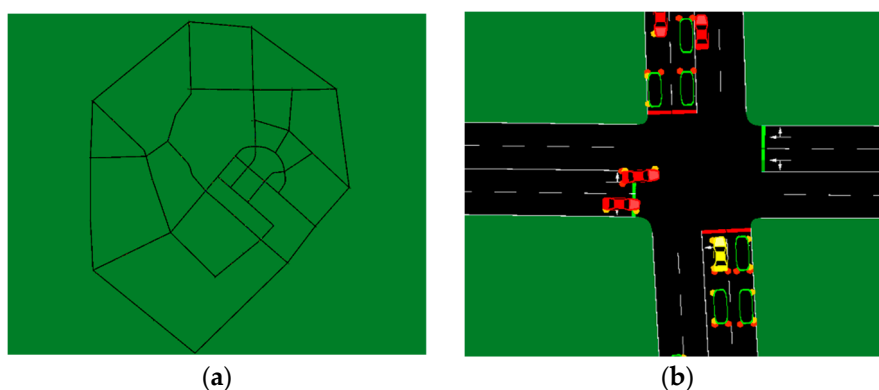


Figure 3. Traffic network model based on the simulation of urban mobility (SUMO) software: (a) map of the 20 km² area; (b) local intersection model.

The traffic network parameters are set according to the observation data as listed in Table 3. By continuously adjusting the traffic model parameters manually, the traffic flow data of the traffic model is close to the observed data. Finally, we get the manually set origin-destination matrix (OD Matrix) as listed in Matrix (17); the value (x, y) of the matrix represents vehicles per hour from the starting point x to the end point y. The value of (x, y) is manually adjusted based on the observed data in Table 3.

$$\begin{bmatrix}
 0 & 40 & \dots & 4 & 21 \\
 100 & 0 & \dots & 110 & 30 \\
 \dots & \dots & 0 & \dots & \dots \\
 200 & 220 & \dots & 0 & 150 \\
 190 & 460 & \dots & 260 & 0
 \end{bmatrix} \tag{17}$$

Table 3. Actual observed traffic data.

Data Observation	Value
Number of roads	3
Observation period	Monday to Friday 16:30–17:30
Average traffic flow	380 vehicles/min
Average traffic density	80 vehicles/km
Average speed	34 km/h

According to the proportion of the vehicles on the actual road, the proportion of each type of vehicle is set as Table 4. In the traffic model, the vehicle-following model of each type of vehicle is defined according to the vehicle-following model recommended by the SUMO software. Python controls the SUMO run and sets the parameters in the SUMO simulation through the TraCI [28] interface protocol and the traffic data generated by the SUMO simulation can also be accessed in Python for the next step of data processing.

Table 4. The proportion of each vehicle type in the traffic simulation model.

Vehicle Type	Value
Fuel family vehicle	50%
EV	10%
Bus	10%
Taxi	20%
Truck	8%
Cleaning vehicle	2%

The vehicle model is put into the road network of the traffic simulation model for joint simulation, and the traffic information data and the driving condition data set of EVs are obtained. The data set lays a foundation for the energy consumption prediction model.

4. A Prediction of EV Energy Consumption Integrating Traffic Information and Driving Data

For the traditional EV energy consumption prediction, they usually simulate the EV with the driving condition of the NEDC cycle or the constant speed of 60 km/h based on the remaining energy and estimate the remaining driving range. However, this method would result in an inaccurate estimation due to the difference in actual driving. Therefore, an EV energy consumption prediction method that considers traffic information is put forward. This method replaces the NEDC driving cycle or the constant speed 60 km/h driving condition with the actual traffic environment and integrates traffic information and vehicle driving condition information, which makes the prediction of the driving energy consumption of EV more accurate. Because LSTM [29] has a special gating structure, it largely overcomes the shortcomings of the traditional recurrent neural network (RNN) [30] that the data memory of long-term sequences is not strong enough. While EV driving condition data and traffic information data are just typical domain data, here, we use the LSTM, as shown in Figure 4 to establish a deep learning-based EV energy consumption prediction model.

Where in Figure 4, X_t is the input of the current time, h_{t-1} is the output of the previous LSTM unit, C_{t-1} is the memory of the previous unit, the output of the current network is h_t , and C_t is the memory of the current unit. LSTM's forgotten gate is responsible for forgetting part of the content and the selective input gate selects part of h_{t-1} and X_t in order to avoid over-fitting of the model. The selective output gate implements the selective output of the internal data of the LSTM model.

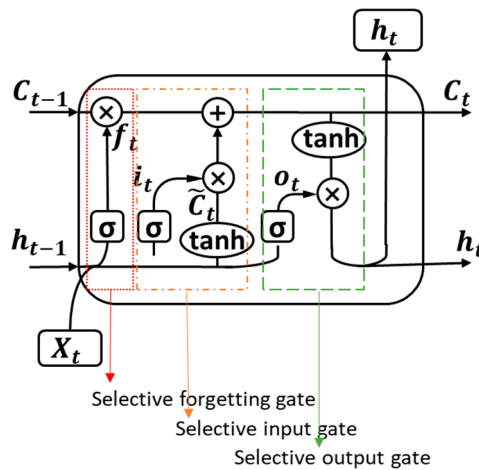


Figure 4. Long-term, short-term memory neural network (LSTM) schematic diagram with selective structure.

Based on LSTM, an EV energy consumption prediction model based on traffic information and vehicle driving condition information as listed in Table 5 is established, as shown in Figure 5. The sequence to sequence technology is used to realize the fusion of multi-dimensional data from transportation and electric vehicles and the result of data fusion serves as an input to LSTM. Sequence to sequence is a technique for implementing data mapping from one-dimensional sequence to another that is not the same as the original data dimension. The model takes the data as a sequence node every five minutes, takes the historical data of the first fifty-five minutes as input, and outputs the driving energy consumption of each electric vehicle in the traffic network in the next five minutes.

Table 5. Training data for the LSTM model.

Traffic Information Data	Electric Vehicle Driving Condition Data
Link length	SOC ₀
Average speed	Road energy consumption
Average traffic flow	Battery voltage
Average traffic density	Battery current

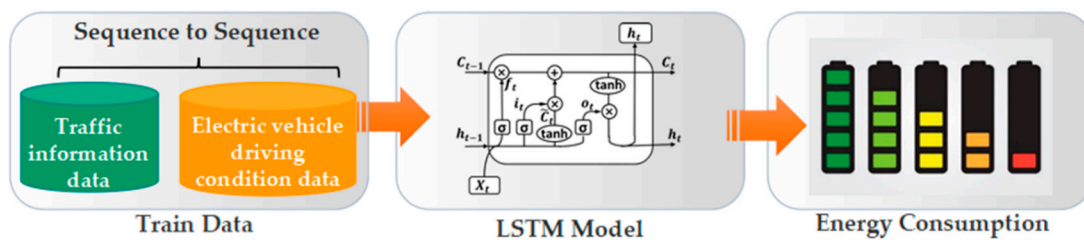


Figure 5. The framework of the EV energy consumption prediction model.

After finishing the LSTM model training, the model error is verified using the mean absolute error (MAE) and mean square error (MSE), respectively. Using experiments, the comparison variable is the number of roads in the training data, the simulation duration, and the results are listed in Tables 6 and 7 and shown in Figures 6–11.

Table 6. The influence of the number of roads in the model input data on the prediction results.

Road Number	Road Share	Simulation Time	MAE	MSE
33	25%	6 h	0.1159	0.0217
65	50%	6 h	0.1133	0.0196
130	100%	6 h	0.1042	0.0177

Table 7. The influence of different simulation durations in the model input data on the prediction results.

Road Number	Simulation Time	Simulation Time Ratio	MAE	MSE
130	2 h	33.3%	0.1091	0.0208
130	4 h	66.7%	0.1048	0.0184
130	6 h	100%	0.1042	0.0177

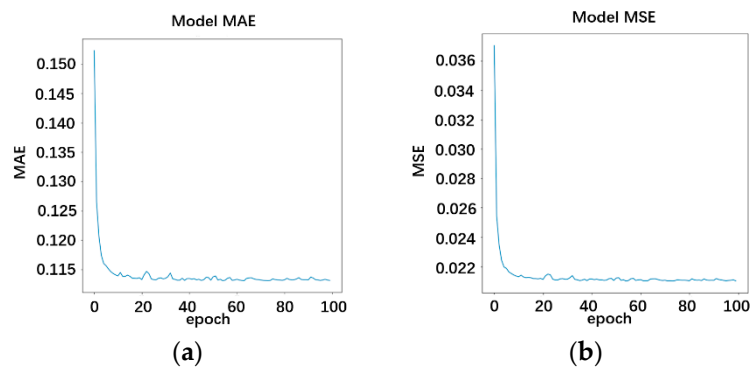


Figure 6. Model training error of 25% road quantity: (a) model mean absolute error (MAE); (b) model mean square error (MSE).

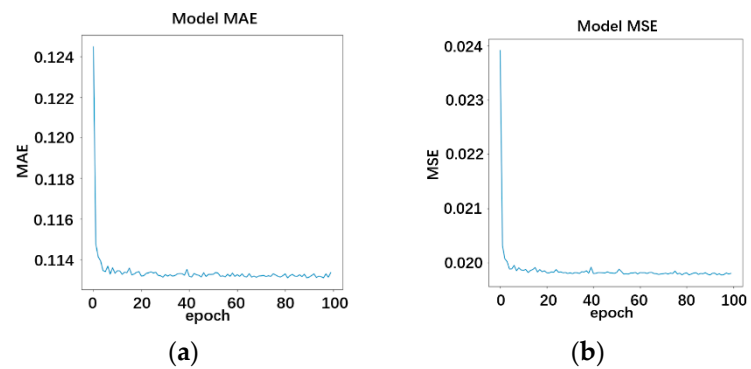


Figure 7. Model training error of 50% road quantity: (a) model MAE; (b) model MSE.

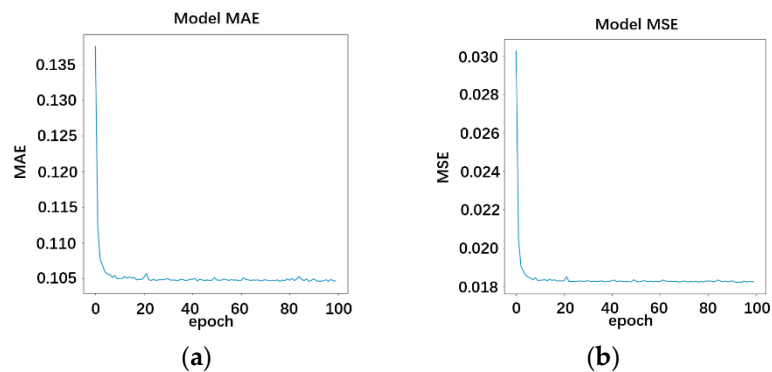


Figure 8. Model training error of 100% road quantity: (a) model MAE; (b) model MSE.

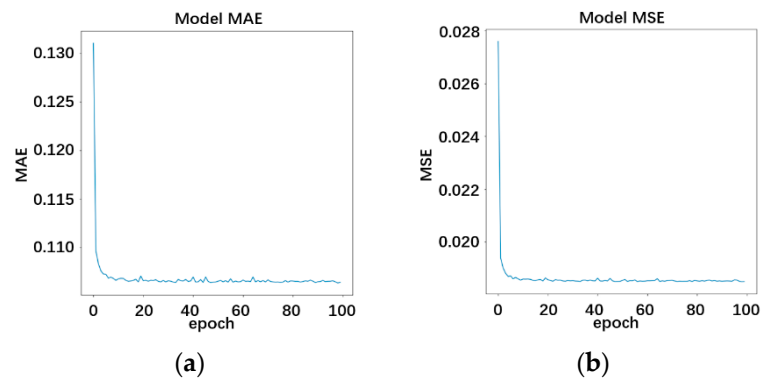


Figure 9. Model error of 2 h simulation data as training data: (a) model MAE; (b) model MSE.

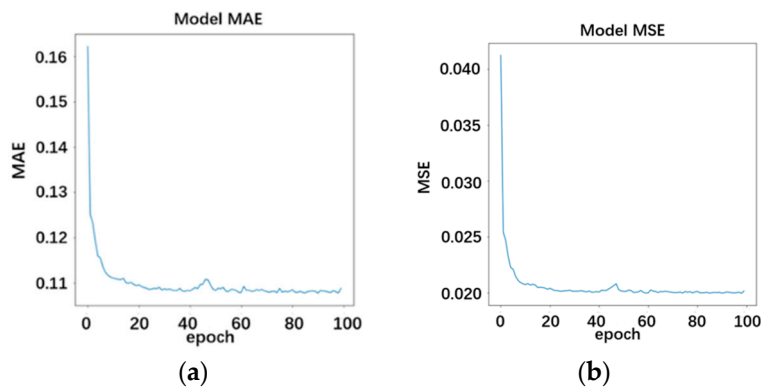


Figure 10. Model error of 4 h simulation data as training data: (a) model MAE; (b) model MSE.

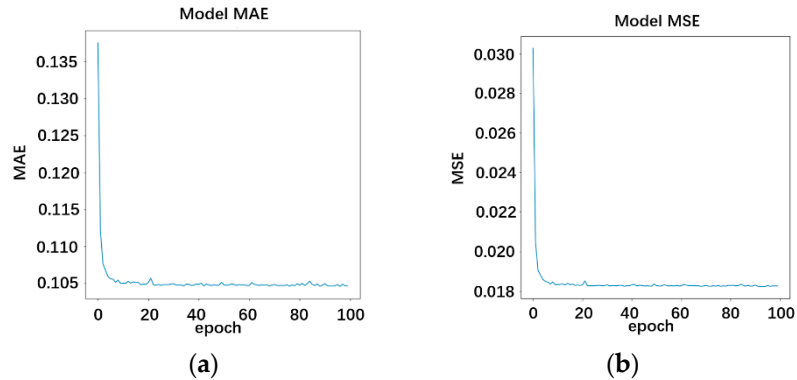


Figure 11. Model error of 6 h simulation data as training data: (a) model MAE; (b) model MSE.

From the experimental results, the error of the LSTM model decreases with the increase of the data duration or the number of roads. When the model input is 6 h and the number of roads is 130, the error is the smallest. In the actual situation, if the training data contains more roads and longer data lengths, the model error will be much smaller. The energy consumption of the electric vehicle on each road can be updated every five minutes according to the changes of traffic conditions and the state of the electric vehicle.

5. The Planning Strategy of the Optimal Coupling Path between Energy Consumption and Distance

After finishing the energy consumption prediction of the electric vehicle, it is also necessary to construct a road resistance cost function to couple the energy consumption with the distance as shown in Equations (18)–(20). In the road resistance function, the weight of the energy consumption and the distance are both set to 50%.

$$f(x_1, x_2, t) = a \times m_{x_1, x_2, t} + b \times n_{x_1, x_2} \quad (18)$$

$$m_{x_1, x_2, t} = g(x_1, x_2, t) \quad (19)$$

$$t = 5 \times q(\text{min}), q = 1, 2, \dots, N \quad (20)$$

where $m_{x_1, x_2, t}$ is the energy consumption of road x_1 to road x_2 at time t , n_{x_1, x_2} is the distance of road x_1 to road x_2 , and a and b are the weighting factors, $a = b = 50\%$. Since the energy consumption of road x_1 to road x_2 changes with time, and the road traffic information changes little in the 5 min time interval, this paper uses 5 min to calculate the energy consumption in one time unit, so q is the number of five minutes after departure. So the energy consumption m is a function of the starting point, the end point and the time. $f(x_1, x_2, t)$ is the road resistance cost function for energy consumption and distance.

The road resistance cost function matrix for this condition can be built as Equation (21)

$$\begin{bmatrix} \infty & f(x_1, x_2, t) & \dots & f(x_1, x_{129}, t) & f(x_1, x_{130}, t) \\ f(x_2, x_1, t) & \infty & \dots & f(x_2, x_{129}, t) & f(x_2, x_{130}, t) \\ \dots & \dots & \infty & \dots & \dots \\ f(x_{129}, x_1, t) & f(x_{129}, x_2, t) & \dots & \infty & f(x_{129}, x_{130}, t) \\ f(x_{130}, x_1, t) & f(x_{130}, x_2, t) & \dots & f(x_{130}, x_{129}, t) & \infty \end{bmatrix} \quad (21)$$

We also set the path of optimal energy consumption and time relative to the path with the shortest energy consumption and distance. The road resistance cost function is shown in Equations (22)–(25).

$$z(x_1, x_2, t) = c \times m_{x_1, x_2, t} + d \times T_{x_1, x_2, t} \quad (22)$$

$$T_{x_1, x_2, t} = n_{x_1, x_2} / v_{avg, x_1, x_2, t} \quad (23)$$

where $T_{x_1, x_2, t}$ is the traveling time needed from x_1 to x_2 at time t . The weighting factors c, d here we set $c = 20\%, d = 80\%$, because usually, people need less travel time than energy consumption. The time t and energy consumption $m_{x_1, x_2, t}$ are defined in Equations (19) and (20). $z(x_1, x_2, t)$ is the road resistance cost function for energy consumption and travel time.

The road resistance cost function matrix for this condition can be built as Equation (24).

$$\begin{bmatrix} \infty & z(x_1, x_2, t) & \dots & z(x_1, x_{129}, t) & z(x_1, x_{130}, t) \\ z(x_2, x_1, t) & \infty & \dots & z(x_2, x_{129}, t) & z(x_2, x_{130}, t) \\ \dots & \dots & \infty & \dots & \dots \\ z(x_{129}, x_1, t) & z(x_{129}, x_2, t) & \dots & \infty & z(x_{129}, x_{130}, t) \\ z(x_{130}, x_1, t) & z(x_{130}, x_2, t) & \dots & z(x_{130}, x_{129}, t) & \infty \end{bmatrix} \quad (24)$$

A-Star algorithm is a heuristic algorithm, as shown in Figure 12, which can determine the search scope based on the estimated value of the current point-to-end road resistance, making the search point closer and closer to the optimal point. A-Star algorithm is widely used in the scenarios of autonomous driving path planning and vehicle navigation [31]. Here we select the A-Star algorithm as the main solver, the road resistance and the traffic network obtained by the above equations are taken as inputs like matrix (21) and matrix (24), and the A-Star algorithm can output the best driving path. Take the energy consumption and driving distance as optimization goals, or take energy consumption and driving time as optimization goals to plan the economic driving path.

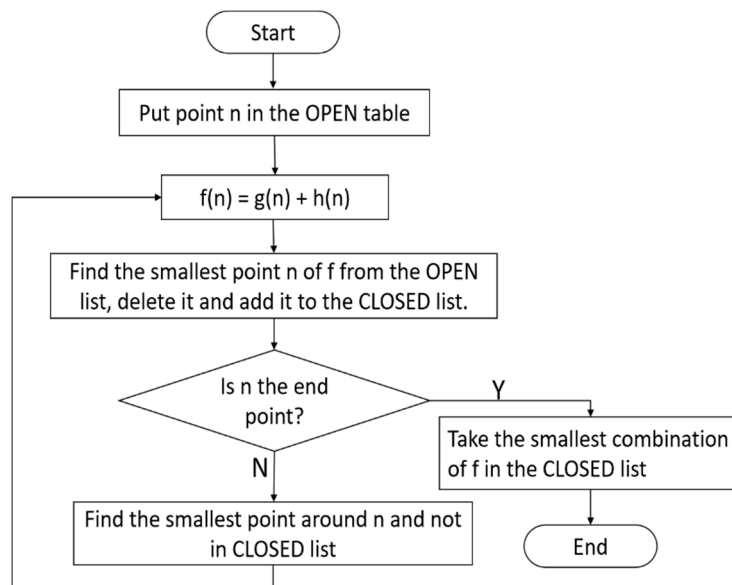


Figure 12. A-Star Algorithm.

6. Results and Discussion

In this paper, three groups of experiments are set up, that is, distance-based, energy-based, and time-based optimal simulation experiments. The optimal distance path is used as the comparison base. The experiment of coupling the optimization of energy consumption and distance and the experiment of time optimization and energy consumption optimization are used to prove the application value of energy consumption prediction considering the traffic information in path planning.

According to the experiment results as shown in Figure 13 and Table 8, the shortest distance-based optimization path from the starting point to the end point is 3515.3 m, the EV consumes 0.731 kWh electricity with the equivalent energy consumption rate of 20.79 kWh/100 km and the average speed is 16.17 km/h, indicating that the road is relatively congested and the energy consumption is relatively high. For the coupling optimal energy consumption and distance path, here named as the energy saving-based optimization path, the total electricity consumption is 0.686 kWh with an equivalent energy consumption rate of 18.73 kWh/100 km, 9.9% less than the shortest distance-based optimization path and is the lowest energy consumption among the three paths. For the coupling optimal energy consumption and time path, here named as the time saving-based optimization path, its driving time is 5.9 min and is the shortest time consumption path, while its total electricity consumption is 0.705 kWh with the equivalent energy consumption rate of 19.03 kWh/100 km, 8.4% less than the shortest distance-based optimization path and 1.6% more than the energy saving-based optimization path.

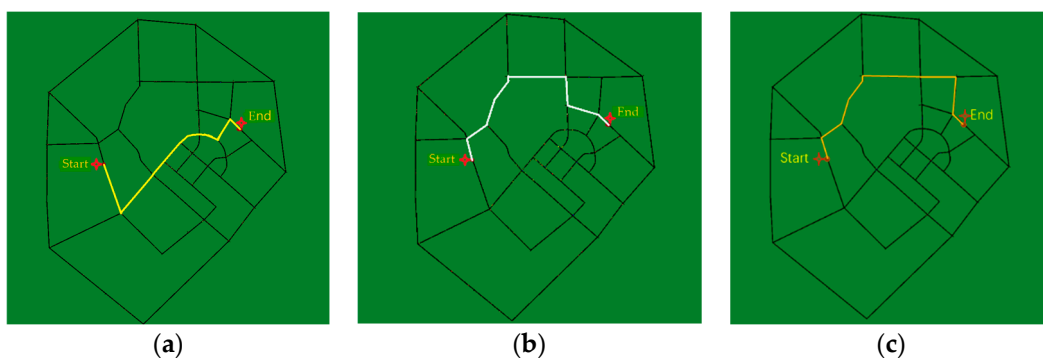


Figure 13. The optimal path results with different targets: (a) the shortest distance-based optimal path; (b) the energy saving-based optimal path; (c) the time saving-based optimization path.

Table 8. The optimal results for different optimization conditions.

Path Type	Drive Distance	Energy Consumption	Equivalent Energy Consumption Rate	Traveling Time	Average Speed
Shortest Distance-based	3515.3 m	0.731 kWh	20.79 kWh/100 km	11.7 min	16.17 km/h
Energy saving-based	3661.8 m	0.686 kWh	18.73 kWh/100 km	7.0 min	31.39 km/h
Time saving-based	3705.6 m	0.705 kWh	19.03 kWh/100 km	5.9 min	37.68 km/h

7. Conclusions

- (1) The EV energy consumption model is built and verified through a test bench experiment of 3 NEDC driving cycles and actual road driving cycles. The actual traffic network is modeled with the software SUMO updated with actual traffic data. In order to predict the energy consumption accurately, a deep learning-based energy consumption prediction model with LSTM is proposed, which can fuse multi-dimensional data from different sources including traffic information. The sequence to sequence technology is used to realize the fusion of multi-dimensional data from transportation and electric vehicles. The dimensions and influence of the model training input data are also discussed with the result of 6 h long and 130 roads minimum.
- (2) A path planning map and the road resistance function are established, and the energy-saving path planning strategy with the optimal coupling of energy consumption and distance or energy consumption and driving time is proposed by the usage of the A-star algorithm. As a comparison, the shortest distance-based optimal path is also performed. The comparison results show that for the coupling optimal energy consumption and distance path, its equivalent energy consumption rate is 9.9% less than the shortest distance-based optimization path, while for the coupling optimal energy consumption and time path, it is 8.4% less than the shortest distance-based optimization path.

Author Contributions: H.H., J.L., and G.Z. conceived and designed the paper idea; J.L. and Q.L. performed the experiments; J.L. wrote the paper and H.H. revised the paper.

Funding: This research was funded by the National Key R&D project of China (Grand No. 2017YFB0103701).

Acknowledgments: The authors would like to thank the reviewers for their corrections and helpful suggestions.

Conflicts of Interest: The authors declare no conflict of interest.

References

1. Ke, W.; Zhang, S.; He, X.; Wu, Y.; Hao, J. Well-to-wheels energy consumption and emissions of electric vehicles: Mid-term implications from real-world features and air pollution control progress. *Appl. Energy* **2017**, *188*, 367–377. [[CrossRef](#)]
2. Roy, J.V.; Leemput, N.; Geth, F.; Büscher, J.; Salenbien, R.; Driesen, J. Electric Vehicle Charging in an Office Building Microgrid With Distributed Energy Resources. *IEEE Trans. Sustain. Energy* **2017**, *5*, 1389–1396.
3. Hu, J.; Zheng, L.; Jia, M.; Zhang, Y.; Pang, T. Optimization and Model Validation of Operation Control Strategies for a Novel Dual-Motor Coupling-Propulsion Pure Electric Vehicle. *Energies* **2018**, *11*, 754. [[CrossRef](#)]
4. Marotta, A.; Pavlovic, J.; Ciuffo, B.; Serra, S.; Fontaras, G. Gaseous Emissions from Light-Duty Vehicles: Moving from NEDC to the New WLTP Test Procedure. *Environ. Sci. Technol.* **2015**, *49*, 8315–8322. [[CrossRef](#)]
5. Alizadeh, M.; Wai, H.T.; Scaglione, A.; Goldsmith, A.; Fan, Y.Y.; Javidi, T. Optimized path planning for electric vehicle routing and charging. In Proceedings of the Communication, Control, Computing, Monticello, IL, USA, 30 September–3 October 2014.
6. Hoch, N.; Zemmer, K.; Werther, B.; Siegwart, R.Y. Electric vehicle travel optimization-customer satisfaction despite resource constraints. In Proceedings of the IEEE Intelligent Vehicles Symposium, Alcalá de Henares, Spain, 3–7 June 2012.
7. Montazeri-Gh, M.; Mahmoodi-K, M. Optimized predictive energy management of plug-in hybrid electric vehicle based on traffic condition. *J. Clean. Prod.* **2016**, *139*, 935–948.

8. Fiori, C.; Ahn, K.; Rakha, H.A. Power-based electric vehicle energy consumption model: Model development and validation. *Appl. Energy* **2016**, *168*, 257–268. [[CrossRef](#)]
9. Xiang, C.; Ding, F.; Wang, W.; He, W. Energy management of a dual-mode power-split hybrid electric vehicle based on velocity prediction and nonlinear model predictive control. *Appl. Energy* **2017**, *189*, 640–653. [[CrossRef](#)]
10. Vaz, W.; Nandi, A.K.; Landers, R.G.; Koyle, U.O. Electric vehicle range prediction for constant speed trip using multi-objective optimization. *J. Power Sources* **2015**, *275*, 435–446. [[CrossRef](#)]
11. Sun, C.; Sun, F.; He, H. Investigating adaptive-ECMS with velocity forecast ability for hybrid electric vehicles. *Appl. Energy* **2017**, *185*, 1644–1653. [[CrossRef](#)]
12. Zhang, S.; Luo, Y.; Wang, J.; Wang, X.; Li, K. Predictive energy management strategy for fully electric vehicles based on preceding vehicle movement. *IEEE Trans. Intell. Transp. Syst.* **2017**, *18*, 3049–3060. [[CrossRef](#)]
13. Qiu, L.; Qian, L.; Zomorodi, H.; Pisu, P. Global optimal energy management control strategies for connected four-wheel-drive hybrid electric vehicles. *IET Intell. Transp. Syst.* **2017**, *11*, 264–272. [[CrossRef](#)]
14. Qi, X.; Wu, G.; Boriboonsomsin, K.; Barth, M.J.; Gonder, J. Data-Driven Reinforcement Learning-Based Real-Time Energy Management System for Plug-In Hybrid Electric Vehicles. *Transp. Res. Rec.* **2016**, *2572*, 1–8. [[CrossRef](#)]
15. Shan, X.N.; Hao, P.; Chen, X.H.; Boriboonsomsin, K.; Wu, G.Y.; Barth, M.J. Vehicle Energy/Emissions Estimation Based on Vehicle Trajectory Reconstruction Using Sparse Mobile Sensor Data. *IEEE Trans. Intell. Transp. Syst.* **2019**, *20*, 716–726. [[CrossRef](#)]
16. Qi, X.; Wu, G.; Boriboonsomsin, K.; Barth, M.J. Data-driven decomposition analysis and estimation of link-level electric vehicle energy consumption under real-world traffic conditions. *Transp. Res. Part D—Transp. Environ.* **2018**, *64*, 36–52. [[CrossRef](#)]
17. Qi, X.; Wu, G.; Boriboonsomsin, K.; Barth, M.J. Development and Evaluation of an Evolutionary Algorithm-Based Online Energy Management System for Plug-In Hybrid Electric Vehicles. *IEEE Trans. Intell. Transp. Syst.* **2017**, *18*, 2181–2191. [[CrossRef](#)]
18. Robinson, A.P.; Blythe, P.T.; Bell, M.C.; Hübner, Y.; Hill, G.A. Analysis of electric vehicle driver recharging demand profiles and subsequent impacts on the carbon content of electric vehicle trips. *Energy Policy* **2013**, *61*, 337–348. [[CrossRef](#)]
19. Sajadi-Alamdari, S.A.; Voos, H.; Darouach, M. Fast stochastic non-linear model predictive control for electric vehicle advanced driver assistance systems. In Proceedings of the IEEE International Conference on Vehicular Electronics and Safety, Vienna, Austria, 27–28 June 2017.
20. He, H.; Xiong, R.; Fan, J. Energies, Vol. 4, Pages 582-598: Evaluation of Lithium-Ion Battery Equivalent Circuit Models for State of Charge Estimation by an Experimental Approach. *Energies* **2011**, *4*, 582–598. [[CrossRef](#)]
21. Cordoba-Arenas, A.; Onori, S.; Guezennec, Y.; Rizzoni, G. Capacity and power fade cycle-life model for plug-in hybrid electric vehicle lithium-ion battery cells containing blended spinel and layered-oxide positive electrodes. *J. Power Sources* **2015**, *278*, 473–483. [[CrossRef](#)]
22. Mousavi MS, R.; Pakniyat, A.; Tao, W.; Boulet, B. Seamless dual brake transmission for electric vehicles: Design, control and experiment. *Mech. Mach. Theory* **2015**, *94*, 96–118. [[CrossRef](#)]
23. Bo, L.; Lim, S.T.; Zhi, F.B.; Ryu, J.H.; Chong, K.T. Energy Management and Control of Electric Vehicles, Using Hybrid Power Source in Regenerative Braking Operation. *Energies* **2014**, *7*, 4300–4315.
24. Xia, B.; Wang, H.; Yong, T.; Wang, M.; Sun, W.; Xu, Z. State of Charge Estimation of Lithium-Ion Batteries Using an Adaptive Cubature Kalman Filter. *Energies* **2015**, *8*, 5916–5936. [[CrossRef](#)]
25. Zhang, D.H.; Qiu, S.; Zhu, G.R.; He, S.J.; Ma, Y.; Wu, Q.M.; Chen, W. Balancing a Control Strategy for a Li-Ion Batteries String Based on the Dynamic Balanced Point. *Energies* **2015**, *8*, 1830–1847. [[CrossRef](#)]
26. Fernández-Yáñez, P.; Armas, O.; Martínez-Martínez, S. Impact of relative position vehicle-wind blower in a roller test bench under climatic chamber. *Appl. Therm. Eng.* **2016**, *106*, 266–274. [[CrossRef](#)]
27. Azevedo, T.; De Araújo, P.J.M.; Rossetti, R.J.F.; Rocha, A.P.C. JADE, TraSMAPI and SUMO: A tool-chain for simulating traffic light control. *arXiv* **2014**, arXiv:1601.08154.
28. Ahmed, M.S.; Hoque, M.A. Partitioning of urban transportation networks utilizing real-world traffic parameters for distributed simulation in SUMO. In Proceedings of the IEEE Vehicular Networking Conference, Torino, Italy, 27–29 November 2017.

29. Greff, K.; Srivastava, R.K.; Koutnik, J.; Steunebrink, B.R.; Schmidhuber, J. LSTM: A Search Space Odyssey. *IEEE Trans. Neural Netw. Learn. Syst.* **2016**, *28*, 2222–2232. [[CrossRef](#)] [[PubMed](#)]
30. Cho, K.; Van Merriënboer, B.; Gulcehre, C.; Bahdanau, D.; Bougares, F.; Schwenk, H.; Bengio, Y. Learning Phrase Representations using RNN Encoder-Decoder for Statistical Machine Translation. *Comput. Sci.* **2014**, arXiv:1406.1078.
31. Liu, C.G.; Mao, Q.Z.; Chu, X.M.; Xie, S. An improved A-star Algorithm Considering Water Current, Traffic Separation and Berthing for Vessel Path Planning. *Appl. Sci.* **2019**, *9*, 1057. [[CrossRef](#)]



© 2019 by the authors. Licensee MDPI, Basel, Switzerland. This article is an open access article distributed under the terms and conditions of the Creative Commons Attribution (CC BY) license (<http://creativecommons.org/licenses/by/4.0/>).